# Gain Enhancement Using Modified Circular Loop FSS Loaded with Slot Antenna for Sub-6 GHz 5G Application

**Anubhav Kumar[1, *], Asok De[2], and Rakesh K. Jain[1]**

**Abstract**—In this paper, a modified circular loop Frequency Selective Surface (FSS) loaded on a slot antenna is proposed for sub-6 GHz 5G applications. The proposed FSS reduces the resonant frequency to lower bands of conventional circular FSS without change in its size. The operating bandwidth ($-10$ dB) of the proposed antenna with polarization-insensitive single-layer FSS varies from 3.6 GHz to 6.1 GHz with an average gain of 7–7.5 dB and a maximum realized gain of 7.87 dB. An FSS superstrate is loaded onto a slot antenna to increase the realized gain up to 4 dB, where the FSS shows desirable electromagnetic wave reflection characteristics over operating bandwidth and can be used in 5G sub-6 GHz band applications.

## 1. INTRODUCTION

Frequency selective surface (FSS) structure is used for gain, bandwidth enhancement and grating lobe reduction in microstrip antenna, which can reflect or pass the EM waves coming from the antenna. Several gain enhancement techniques have been investigated to enhance the properties of microstrip antenna such as artificial magnetic conductor (AMC) [5], metamaterial [1, 6, 13], single [8, 10], and double-layer FSS [2, 7, 11]. In [1], a double split ring reflector based on mu-negative characteristic of the metasurface is used for gain enhancement. The dual FSS layers based on stopband reflector are loaded on a ultra-wideband (UWB) antenna, where a split ring in the top layer and the combination of Jerusalem cross (JC) FSS with a square loop in the bottom layer are used for gain enhancement [2]. A parabolic cylinder FSS reflector is accomplished on a dielectric resonator antenna (DRA) and monopole antenna to enhance the gain [3]. Due to the tremendous reflecting and absorbing property of FSS, multilayer FSS is also a popular approach for enhancing the parameters of a microstrip antenna. In [4], a multi-layer bandpass FSS placed above the antenna is used to enhance the gain. In [5], a triple band AMC structure is used below the antenna for gain enhancement where AMC represents zero reflection phases in the resonant frequencies. In [6], split-ring resonator (SRR) metamaterial is loaded on a DRA to enhance the gain with stable efficiency in the operating bandwidth. In [7], a double-layer passband FSS is used to influence the gain at ISM band placed over microstrip antenna. In [8], the single-layer passband substrate integrated waveguide (SIW)-FSS is loaded to enhance the gain of a microstrip antenna whereas in [9] an FSS combined with a DRA is used for gain enhancement. In [10], double-side single layer FSS incorporated with chip resistor is used for gain enhancement of a DRA in X-band. Similarly in [11, 12], a double-layer FSS reflector is designed for UWB applications, improving the gain effectively. In [13], a metamaterial SRR incorporated with the antenna in the same substrate is used to enhance the gain in two operating bands. In the proposed paper, a modified circular loop FSS is designed. The insensitive polarization FSS is analyzed for the gain improvement of a slot antenna based on microstrip-feed in sub-6 GHz operating bandwidth.

## 2. ANTENNA DESIGN WITH EQUIVALENT CIRCUIT (EC) MODEL

The proposed slot antenna with fabricated hardware is shown in Fig. 1(a) where dimensions are as follows (in mm): $W1 = 2$, $W3 = 1.5$, $W4 = 0.75$, $W5 = 9$, $W6 = 12$, $W7 = 13.5$, $W8 = 1$, $Ls = 30$, $L1 = 2$, $L2 = 7$, $L3 = 14.5$, $Wf = 3$. FR-4 material is utilized to design the antenna with a 4.4 dielectric constant. The proposed antenna size is $30 \times 30 \times 1.6\,\text{mm}^3$, which is based on a microstrip-fed and slot based defected ground. In the first step as model-I, 15 mm length ($Lf$) of microstrip-fed line with 3 mm width ($Wf$) is used for achieving 50-ohm impedance where the length of the microstrip-fed is directly related to the operating bandwidth. A rectangular slot is inserted in the ground as Model-I in Fig. 1(b) that influences the impedance matching which results in impedance bandwidth ($-10\,\text{dB}$) from 3.4 GHz to 4 GHz as depicted in Fig. 1(c). In the second step as model-II, the internal impedance of an antenna is influenced by the variation of the ground, when the size of the rectangular slot of the ground increases and tilted $45°$, which enhances the impedance bandwidth from 3.5 GHz to 5.9 GHz. In the last step, inductance width increases with some corner defect in the ground therefore resonant frequency of antenna shifted from 4.8 GHz to 4.7 GHz where impedance bandwidth varies from 3.5 GHz to 6.1 GHz as depicted in Fig. 1(c) in Model-III. The EC model of the proposed antenna is developed and tuned with QUCS software as represented in Fig. 1(d). The $|S_{11}|$ bandwidth of EC model is matched with antenna bandwidth illustrated in Fig. 1(e), where lumped elements of feed line ($Lf$, $Cf$), slot in-ground ($Lg$, $Cg$), and resonant frequency ($Rp$, $Lp$ and $Cp$) are $Lf = 2\,\text{nH}$, $Cf = 0.63\,\text{pF}$, $Lg = 3.7\,\text{nH}$, $Cg = 1.577\,\text{pF}$, $Rp = 49\,\Omega$, $Lp = 1.96\,\text{nH}$, and $Cp = 1.03\,\text{pF}$.

## 3. DESIGN OF THE FREQUENCY SELECTIVE SURFACE

### 3.1. Design of the Unit Cell

The proposed modified circular loop FSS is optimized for a 5G sub-6 GHz application with a stopband characteristic, which varies from 3 GHz to 7.8 GHz. The design steps of a unit cell FSS are illustrated in Fig. 2(a) and discussed as follows:

**Step-I** — The FSS stopband and reflection characteristics depend on unit cell periodicity (P) and the incidence angle ($\theta_o$) of the EM waves coming from the antenna. The periodicity (P) can be calculated by the wavelength ($\lambda$) of the EM waves, and its incidence angle is represented in Equation (1) [17].

$$\mathbf{P} < \frac{\boldsymbol{\lambda}}{\mathbf{1 + \sin\theta_o}} \tag{1}$$

When incident angle varies from $0°$ to $60°$, the FSS unit cell size should not exceed 26.79 mm for a 6 GHz frequency by implementing Equation (1). Therefore, in the first step, the customized size of the circular unit cell is taken 14 mm. The ring FSS circumference will be equal to one wavelength, and the radius should be 10.16 mm for 4.7 GHz [14], but here the circular unit cell FSS radius is taken as 6 mm, keeping the compact size as depicted in Fig. 2(a). The 10 dB bandwidth varies from 5.2 GHz to 6.9 GHz and is represented in Fig. 2(b) with resonance frequency 6.1 GHz.

**Step-II** — In the second step, two strips of 0.5 mm width and 12 mm length ($v$) have been combined with a ring FSS (step-I) to increase the 10 dB impedance bandwidth and reduce the resonant frequency without increasing the size. The impedance bandwidth ($-10\,\text{dB}$) of the hybrid unit cell is achieved from 3.6 GHz to 5.7 GHz with a resonant frequency of 4.7 GHz where stopband frequencies vary from 3 GHz to 7.8 GHz, as illustrated in step-II and its $s$-parameters (in dB) in Fig. 2(a) and Fig. 2(b). The reflection phase ($S_{11}$) of FSS unit cell decreases linearly with increasing frequency. The unit cell of the FSS is analyzed with the master-slave condition in $x$- and $y$-planes and Floquet-port in $z$-plane to investigate the stopband response in different angles and polarizations. FSS polarization stability is important and requires characteristics for practical applications. The resonant frequency of an FSS must be stable on the EM waves coming from different angles and polarizations so that it can properly control the grating lobes. The polarization instability of the hybrid structure unit cell is extracted in $TE/TM$ polarization from $0°$ to $60°$, and its $|S_{21}|$ is depicted in Fig. 2(c) and Fig. 2(d). Modified circular FSS is angular stable at a different angle and polarization at an operating frequency. The lumped element of a square loop FSS is discussed in [15]. The overall values of L and C of the EC model are extracted by Equation (2) and Equation (3). The factor $\pi/2$ in Bc and $\pi/4$ in XL is used because of the circular loop structure

(a)



Model-I     Model-II     Model-III

(b)



(c)



(d)



(e)
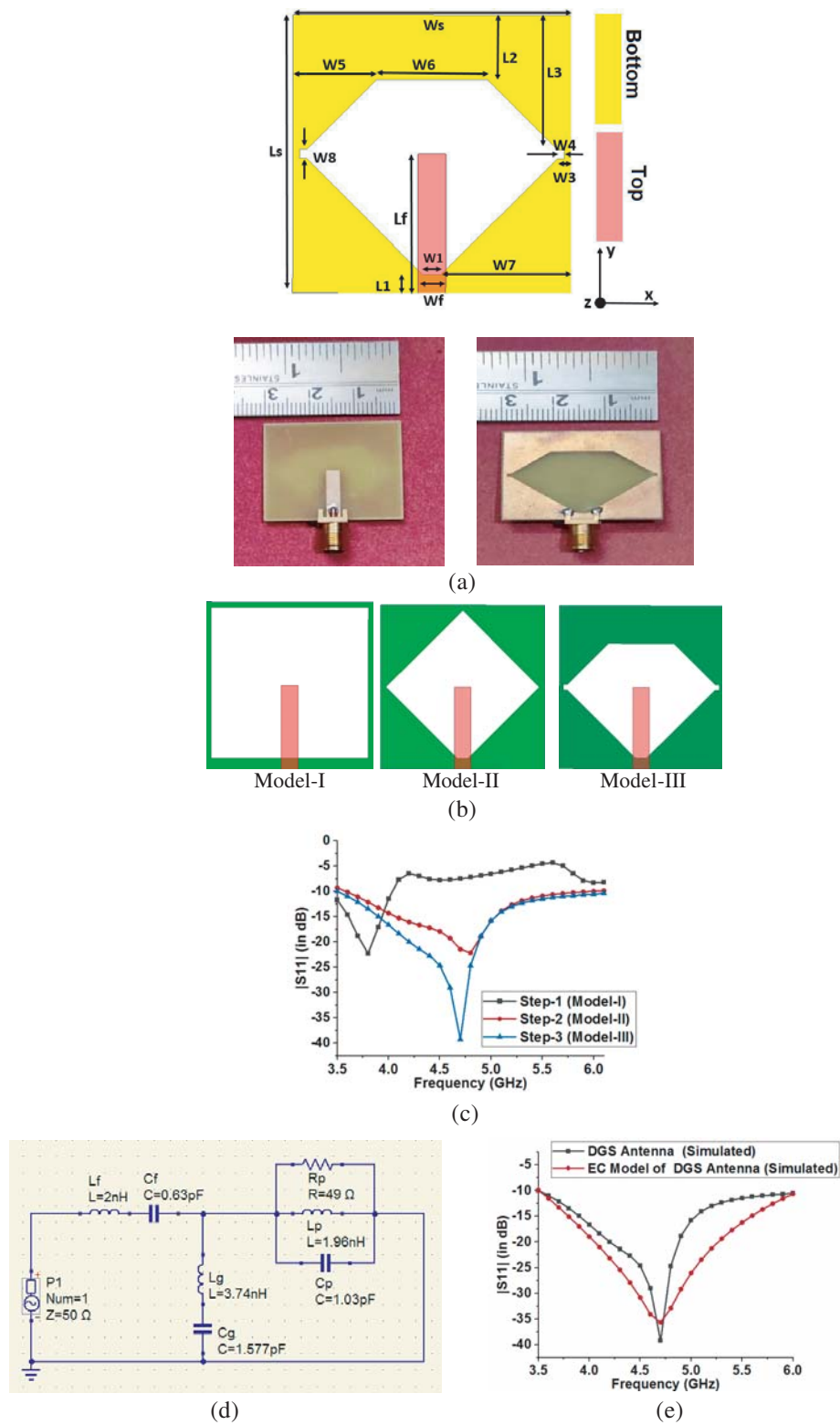
**Figure 1.** (a) Antenna prototype and fabricated antenna. (b) Antenna design steps. (c) $S$-parameters of antenna steps. (d) EC Model. (e) $s$-parameter of EC model and slot antenna.

Step-I                        Step-II

(a)



(b)



(c)



(d)



(e)



(f)
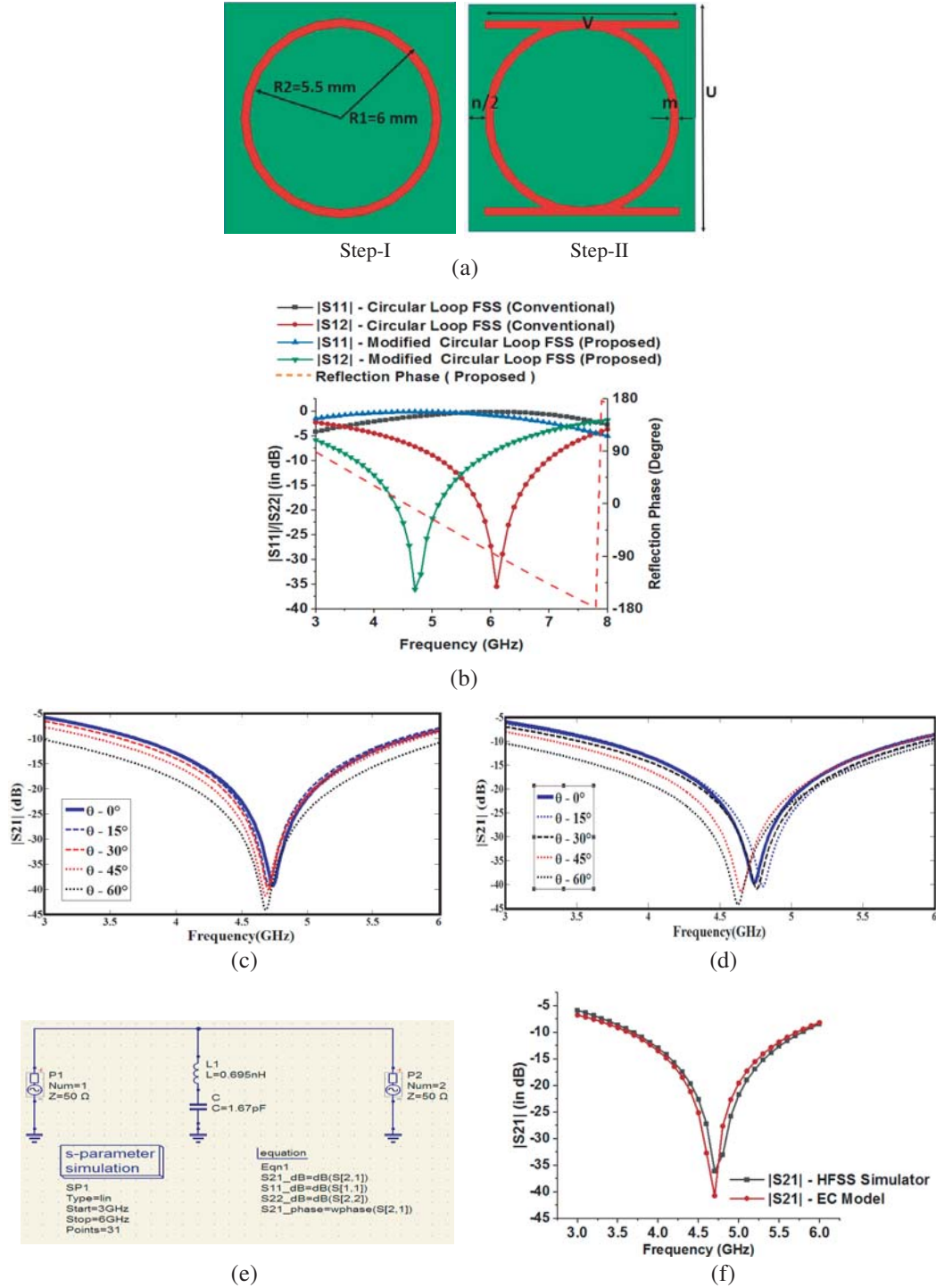
**Figure 2.** Proposed unit cell FSS. (a) Design steps. (b) $s$-parameters. (c) $TE$ polarization. (d) $TM$ polarization. (e) EC model. (f) $s$-parameters of EC model and with EM simulator.

[16]. The lumped elements of the EC model are extracted, and the optimized with QUCS software of the modified circular loop FSS are $L = 0.695$ nH, $C = 1.67$ pF as shown in Fig. 2(e). The EC model and HFSS EM simulation are compared in Fig. 2(f), where the results validate the EC model with the

HFSS simulation.

$$B_c/Y_0 = wC = \frac{\pi}{2} 4\varepsilon_{eff} \frac{V}{U} F(U, n, \lambda, \theta) \tag{2}$$

$$X_L/z_0 = wL = \frac{\pi}{4} \frac{V}{U} F(U, 2m, \lambda, \theta) \tag{3}$$

where $F(U, n, \lambda, \theta)$ and $F(U, 2m, \lambda, \theta)$ can be computed from the

$$F(U, w, \lambda, \theta) = \frac{U}{\lambda} \cos\theta \left[ \ln(\operatorname{cosec} \frac{\pi w}{2U}) \right] + G(U, w, \lambda, \theta) \tag{4}$$

$$G(U, w, \lambda, \theta) = \frac{(1 - \delta^2)^2 \left[ \left(1 - \frac{\delta^2}{4}\right) \left(\frac{A_+ + A_-}{2}\right) + 2\delta^2 A_+ A_- \right]}{\left(1 - \frac{\delta^2}{4}\right) + \delta^2 \left(1 + \frac{\delta^2}{2} - \frac{\delta^4}{8}\right)(A_+ + A_-) + 2\delta^6 A_+ A_-} \tag{5}$$

$$A_\pm = \left[ 1 \pm \frac{2U \sin\theta}{\lambda} - \left(\frac{U \sin\theta}{\lambda}\right)^2 \right]^{-1/2} - 1 \tag{6}$$

and

$$\delta = \sin\left(\frac{\pi w}{2U}\right) \tag{7}$$

## 3.2. Performance Analysis of FSS over Microstrip Antenna

The FSS reflects the unwanted frequency coming from the antenna, and the maximum gain is achieved if the EM waves radiated from the antenna and the EM waves imitated from the FSS are in the same phase. The gain improvement of FSS loaded antenna is dependent upon the reflection phase ($\varphi_{\mathbf{FSS}}$) of FSS and height ($h$) of FSS superstrate from the antenna, extracted from Equation (8).

$$\varphi_{\mathbf{FSS}} - 2\beta\mathbf{h} = 2\mathbf{N}\pi \tag{8}$$

where $\mathbf{N} = 0, 1, 2, 3, \ldots$.

The extracted value of the height of FSS is 32.6 mm from the antenna by Equation (8). The gain enhancement characteristics have been achieved by $7 \times 7$ FSS unit cells with the same material, whereas one unit cell (Modified circular loop FSS) size is $14 \times 14 \times 1.6 \, \text{mm}^3$. The FSS is loaded on a slot antenna with optimized distance as depicted in Fig. 3(a). $|S_{11}|$ in dB and a realized gain of the proposed FSS with a slot antenna are analyzed at different heights ($h$). The $|S_{11}|$ in dB and realized gain of an antenna with different FSS heights from 24.6 to 32.6 mm are presented in Fig. 3(b) and Fig. 3(c). Result reveals that when height of the FSS decreases, $|S_{11}|$ is shifted to the higher frequency due to an increase in coupling between FSS and antenna. The increasing height of FSS leads to decrease in the gain of the antenna at lower frequency and increased gain of the antenna at higher frequency. Higher gain enhancement of the antenna is achieved, when the height of the FSS from the antenna is reduced, but due to the coupling between the antenna and the FSS, the operating bandwidth of the antenna shifts towards higher frequency. Therefore, the optimized distance of the FSS from antenna is considered 28.6 mm. The 10 dB impedance bandwidth (IBW) at 28.6 mm height of FSS varies from 3.6 GHz to 6.1 GHz, which is close to operating frequency (3.5 GHz to 6.1 GHz) of the antenna without FSS. The maximum gain enhancement of 4 dB is achieved at 28.6 mm with less than 1.8 dB variation.

## 4. SIMULATED AND EXPERIMENTS RESULTS

The modified circular loop FSS with a slot antenna is designed on HFSS 13 and measured using Anritsu VNA (MS2038C). The $|S_{11}|$ (in dB) of the slot antenna with and without FSS are illustrated in Fig. 4(a). It is observed from the figure that the antenna exhibits frequency from 3.5 GHz to 6.1 GHz with an absence of FSS and 3.6 GHz to 6.1 GHz with the presence of FSS. The maximum realized gain is achieved as 7.87 dB and 4.3 dB of the proposed slot antenna with the presence and absence of FSS, as illustrated in Fig. 4(b), where the maximum 4 dB gain enhancement is achieved at 5 GHz. The gain

is reduced at 4.9 GHz due to disturbance of the surface current distribution near the feed and slot in the ground. Fig. 4(c) reveals that radiation efficiency (simulated) in the absence and presence of FSS is above 94% throughout the operating frequency band. The co- and cross-polar far-field normalized radiation patterns in $xz$ and $yz$ planes are measured in an anechoic chamber as illustrated in Fig. 4(d) and Fig. 4(e). The co- and cross-polarization difference is higher than 20 dB at resonant frequencies.



(a)



(b)



(c)
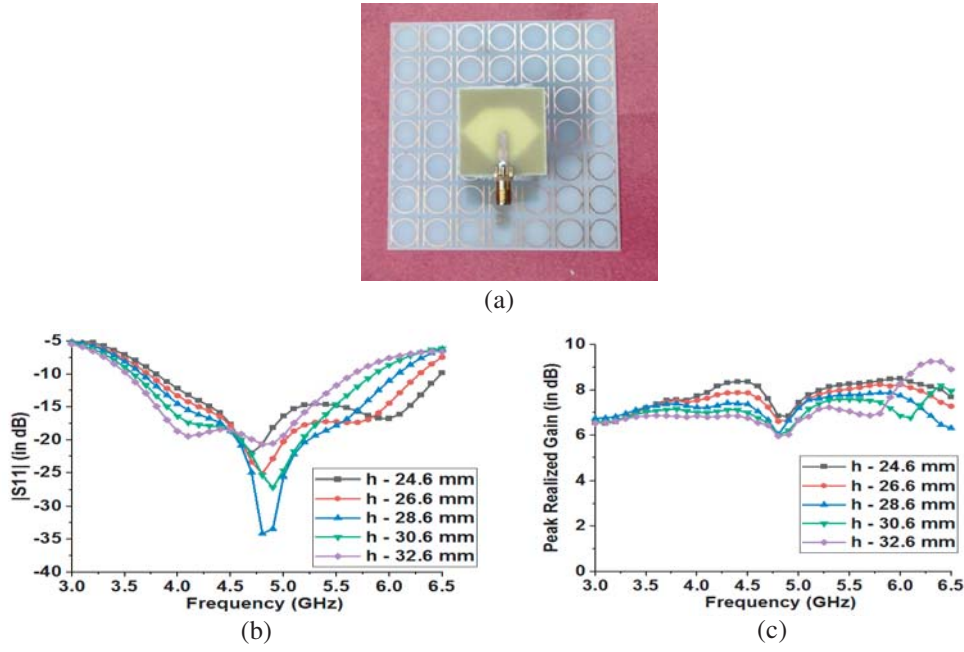
**Figure 3.** Slot antenna loaded at different heights of FSS layer. (a) Hardware prototype of FSS loaded on antenna. (b) $s$-parameters ($|S_{11}|$). (c) Realized gain (dB).



(a)



(b)



(c)

(d)  (e)
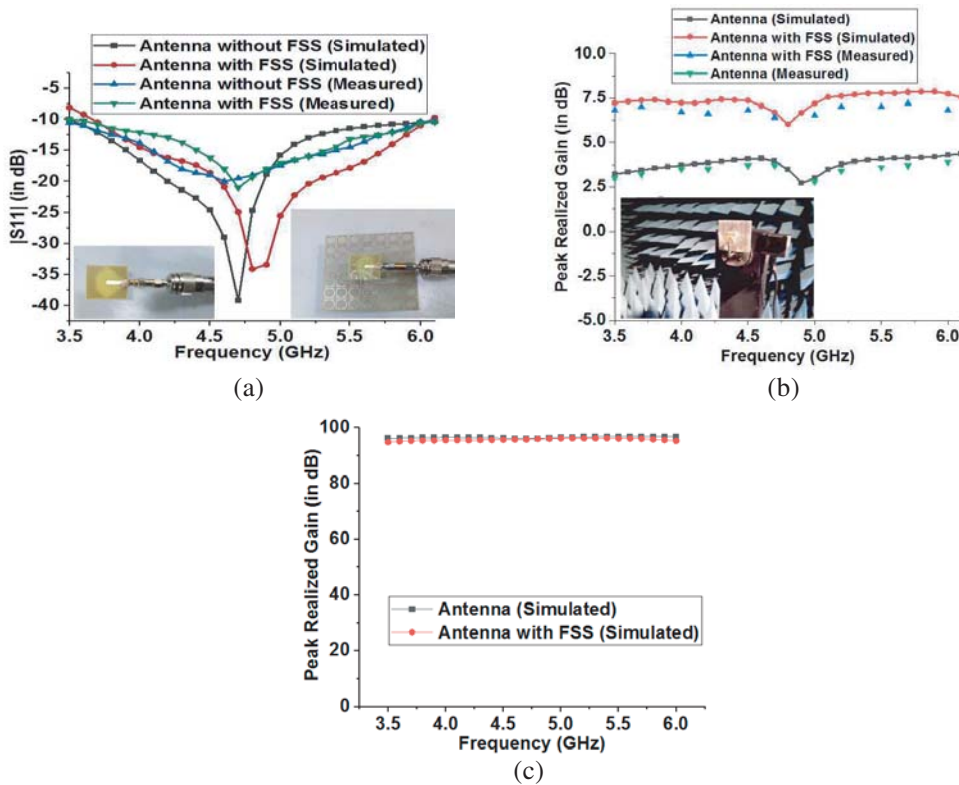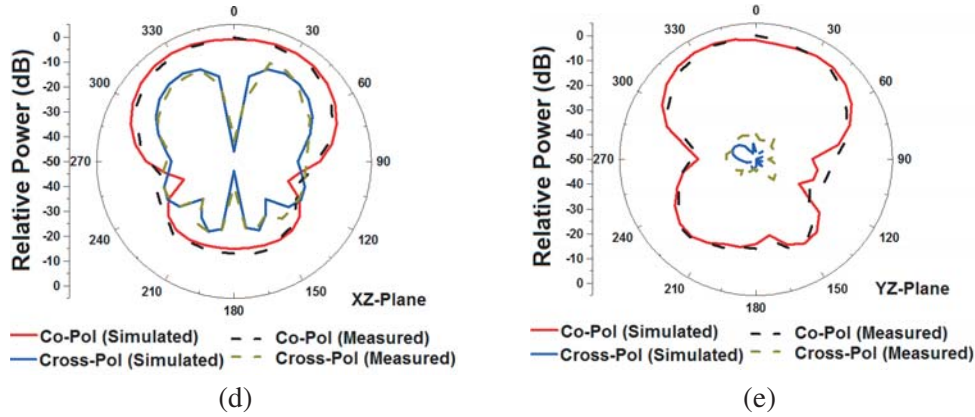
**Figure 4.** Slot antenna results with presence and without FSS. (a) $S$ parameters ($|S_{11}|$ in dB, (b) Realized Gain (in dB). (c) Simulated radiation efficiency (%), Normalized radiation pattern in $xz$ plane (d) and $yz$ plane (e) at 4.7 GHz with FSS.

Table 1 describes the difference between the recently published papers, for gain enhancement. This table concludes that the proposed antenna manifests the 4 dB gain enhancement with a compact size of the antenna and single layer FSS. The maximum gain of the antenna with FSS is about 7.87 dB. Hence, the gain improvement of a slot antenna with a modified circular loop FSS is higher than those given by recently published articles [4, 6, 8–10] with single and dual-layer FSSs, where other articles [5, 7] used higher antenna size or double layer FSS.

**Table 1.** Gain enhancement comparison between proposed antenna and recently published FSS/metasurface papers.

| Reference Nos. | Antenna Dimensions ($mm^3$) | Gain Enhancement Technology | Operating Frequency in GHz (Bandwidth) | Overall Gain | Improvement in gain (dB) |
|---|---|---|---|---|---|
| [4] | $70 \times 70 \times 1.6$ | Band-Pass FSS | 5–8 (3) | 9 | 2–4 |
| [5] | $60 \times 60 \times 1.6$ | AMC | 3.75, 5.98 and 8.79 (Multi-band) | 7.52 | 3.88–4.93 |
| [6] | $60 \times 60 \times 1.6$ | Metamaterial | 5.5–6.5 (1) | 10 | 3 |
| [7] | $63.65 \times 54.16 \times 1.58$ | Band-Pass FSS (Double Layer) | 2.4 | 7 | 5 |
| [8] | $63.65 \times 54.16 \times 1.58$ | SIW FSS | 2.4 | 4.2 | 2 |
| [9] | $50 \times 53.4 \times 1.6$ | DRA-FSS | 2.4 | 5.6 | 3 |
| [10] | $40 \times 30 \times 0.8$ (DR height = 4.3 mm) | FSS (Double side) | 8.15–13.2 (5.05) | 7.8 | 3.3 |
| [11] | $30 \times 60 \times 1.6$ | FSS (Double Layer) | 3.2–12 ( 8.8) | - | 3–4 |
| [12] | $63 \times 63 \times 0.8$ | FSS (Double Layer) | 3–10.6 (7) | 9.8 | 4 |
| **Proposed** | $30 \times 30 \times 1.6$ | **Modified circular loop FSS (Single Layer)** | **3.6 to 6.1 (2.5)** | **7.87** | **4** |

## 5. CONCLUSIONS

This paper presents a modified circular loop FSS loaded with a slot antenna for sub-6 GHz 5G applications. The modified FSS increases the stopband operating bandwidth and shifts it to a lower frequency band without the enhancement of FSS size. The modified FSS is insensitive to the phase change in $TE$ and $TM$ polarization modes. The slot antenna with FSS has obtained a bandwidth from 3.6 GHz to 6.1 GHz with up to 4 dB gain enhancement where the maximum gain of 7.87 dB is achieved.

## REFERENCES

1. Sen, G., A. Banerjee, M. Kumar, and S. Das, "An ultra-wideband monopole antenna with a gain enhanced performance using a novel split-ring meta-surface reflector," *Microwave and Optical Technology Letters*, Vol. 59, No. 6, 1296–1300, 2017.

2. Kundu, S., A. Chatterjee, S. K. Jana, and S. K. Parui, "Gain enhancement of a printed leaf shaped UWB antenna using dual FSS layers and experimental study for ground coupling GPR applications," *Microwave and Optical Technology Letters*, Vol. 60, No. 6, 1417–1423, 2018.

3. Chatterjee, A. and S. K. Parui, "Frequency-dependent directive radiation of monopole-dielectric resonator antenna using a conformal frequency selective surface," *IEEE Transactions on Antennas and Propagation*, Vol. 65, No. 5, 2233–2239, 2017.

4. Chatterjee, A. and K. P. Susanta, "Gain enhancement of a wide slot antenna using a second-order bandpass frequency selective surface," *Radioengineering*, Vol. 24, No. 2, 455–461, 2015.

5. Ghosh, A., T. Mandal, and S. Das, "Design of triple band slot-patch antenna with improved gain using triple band artificial magnetic conductor," *Radioengineering*, Vol. 25, No. 3, 442–448, 2016.

6. Gharsallah, H., L. Osman, and L. Latrach, "Circularly polarized two-layer conical DRA based on metamaterial," *Microwave and Optical Technology Letters*, Vol. 59, No. 8, 1913–1919, 2017.

7. Belen, M. A., "Performance enhancement of a microstrip patch antenna using dual-layer frequency-selective surface for ISM band applications," *Microwave and Optical Technology Letters*, Vol. 60, No. 11, 2730–2734, 2018.

8. Güneş, F., M. A. Belen, and P. Mahouti, "Performance enhancement of a microstrip patch antenna using substrate integrated waveguide frequency selective surface for ISM band applications," *Microwave and Optical Technology Letters*, Vol. 60, No. 5, 1160–1164, 2018.

9. Belen, M. A., P. Mahouti, and M. Palandöken, "Design and realization of novel frequency selective surface loaded dielectric resonator antenna via 3D printing technology," *Microwave and Optical Technology Letters*, Vol. 62, No. 5, 2004–2013, 2020.

10. Bhattacharya, A., B. Dasgupta, and R. Jyoti, "Design and analysis of ultrathin X-band frequency selective surface structure for gain enhancement of hybrid antenna," *International Journal of RF and Microwave Computer-Aided Engineering*, e22505, 2020.

11. Krishna, R. R. and R. Kumar, "Slotted ground microstrip antenna with FSS reflector for high-gain horizontal polarisation," *Electronics Letters*, Vol. 51, No. 8, 599–600, 2015.

12. Ranga, Y., L. Matekovits, K. P. Esselle, and A. R. Weily, "Multioctave frequency selective surface reflector for ultrawideband antennas," *IEEE Antennas Wirel. Propag. Lett.*, Vol. 10, 219–222, 2011.

13. Roy, S. and U. Chakraborty, "Gain enhancement of a dual-band WLAN microstrip antenna loaded with diagonal pattern metamaterials," *IET Communications*, Vol. 12, No. 12 1448–1453, 2018.

14. Huang, J., T.-K. Wu, and S.-W. Lee, "Tri-band frequency selective surface with circular ring elements," *IEEE Transactions on Antennas and Propagation*, Vol. 42, No. 2, 166–175, 1994.

15. Langley, R. J. and E. A. Parker, "Equivalent circuit model for arrays of square loops," *Electronics Letters*, Vol. 18, No. 7, 294–296, 1982.

16. Varkani, A. R., Z. H. Firouzeh, and A. Z. Nezhad, "Equivalent circuit model for array of circular loop FSS structures at oblique angles of incidence," *IET Microwaves, Antennas & Propagation*, Vol. 12, No. 5, 749–755, 2017.

17. Das, P. and K. Mandal, "Modelling of ultra-wide stop-band frequency-selective surface to enhance the gain of a UWB antenna," *IET Microwaves, Antennas & Propagation*, Vol. 13, No. 3, 269–277, 2019.